archives
of thermodynamics
Vol. **41**(2020), No. 1, 67–93
DOI: 10.24425/ather.2020.132950

Numerical study of heat transfer and aerodynamic drag of the radiator with lamellar split finning

YURII NIKOLAENKO*
ALEKSANDR BARANYUK
VALERII ROHACHOV
ALEXANDR TEREKH

National Technical University of Ukraine 'Igor Sikorsky Kyiv Polytechnic Institute', Heat-and-Power Engineering Department, 37 Peremohy Av., 03056, Kyiv, Ukraine

Abstract Promising cooling systems for high-power electronic elements are those based on vapor chambers and heat pipes which allow for the local heat flow to be dispersed from the electronic element to a larger surface area of the vapor chamber or the heat pipe. To reduce the thermal resistance of the cooling system, a finned radiator is installed on the outer surface of the vapor chamber or heat pipe. The authors propose a new design of the radiator which increases the heat transfer efficiency. The paper presents results of numerical simulation of heat transfer and aerodynamic resistance of the heat transfer surface with lamellar-split finning. The comparative analysis of heat transfer and aerodynamics was carried out for three types of radiators: with lamellar smooth finning, with lamellar split finning and with the sections of split finning rotated 30° against the air flow. It is shown that cutting the fins and rotating the split sections leads to an increase in heat transfer intensity and increase in aerodynamic resistance. The obtained results may be useful in the design of cooling systems for computer processors, power amplifiers for transmitting modules, energy-saving solid-state light sources, etc.

Keywords: Microelectronic device; Radiator, Lamellar-split finning; Heat transfer, Aerodynamic resistance; Numerical simulation

*Corresponding Author. Email: yunikola@ukr.net

Nomenclature

b	–	the radiator base thickness, m
C_F	–	coefficient accounting for the influence of the relative splitting depth h_c/h and the rotation angle j of the petals
d	–	diameter, m
E	–	fin efficiency
Eu	–	Euler number
F	–	area of the flow cross-section, m^2
F_1, F_2	–	coefficients accounting for the influence of the rotation angle of the petals
H	–	full surface area, m^2
h	–	radiator fin height, m
K_a	–	coefficient accounting for the air pressure
L	–	radiator base size, m
l	–	line length contact, m
Nu	–	Nusselt number
P	–	total power dissipated by the MED, W; wetted perimeter, m
Q	–	heat power, W
q	–	heat flux density, W/m^2
$R_{\Theta acc}$	–	maximum acceptable thermal resistance, K/W
$R_{\Theta CD}$	–	actual thermal resistance, K/W
Re	–	Reynolds number
S	–	heat exchange surface area, m^2
T	–	temperature, K
T_{el}	–	maximum operating temperature of the active element, K
t	–	step between the fins, m
w	–	average flow speed, m/s
x, y, z	–	Cartesian coordinates
ΔP	–	pressure drop, Pa
ΔT	–	temperature difference, K
max	–	maximum value
min	–	minimum value

Greek symbols

α	–	heat transfer coefficient, $W/(m^2K)$
δ	–	radiator fin thickness, m
λ	–	thermal conductivity coefficient, W/(mK)
ν	–	kinematic viscosity coefficient, m^2/s
φ	–	rotation angle, °
ψ	–	finning coefficient

Subscripts

a	–	air
as	–	average surface
b	–	basis
ch	–	channel
c	–	cut

c	–	convective
e	–	equivalent
env	–	environment
f	–	fin
o	–	oncoming flow
out	–	output
r	–	relative
sm	–	smooth
t	–	total

Abbreviations

CFD	–	computational fluid dynamics
MED	–	microelectronic device
RNG	–	renormalisation group
RSM	–	Reynolds stress model
SST	–	shear stress transport

1 Introduction

It is known that the microelectronics devices (MED) are most sensitive to temperature changes in the environment [1–4]. Therefore, it is important to take optimal thermal management into consideration when performing thermophysical design during the development of the equipment intended for operation in a wide temperature range [4–6]. The temperature change does not only affect electrical parameters and characteristics of the device, but also influences reliability of its performance. An increase in the junction temperature of a semiconductor crystal of an electronic component by 10 °C leads to a decrease in its service life by about half [1,2]. Therefore, the effect of high temperature on the parameters of electronics calls for different methods and means of cooling, which would preserve and stabilize the parameters of microelectronics devices within acceptable limits.

Depending on the purpose of MEDs, different methods are used to remove the heat [4–8]: natural cooling (air, fluid), forced air cooling, forced fluid cooling (with or without surface boiling), cooling based on the change in aggregate state of matter, thermoelectric cooling. The efficiency of any of the methods is determined by the heat transfer intensity – the more intense the heat transfer, the more efficient the cooling method and the higher the heat transfer coefficients [1–19].

The easiest method of MED cooling is passive heat removal using radiators with a particular finning design. In natural cooling, drawing heat out of MED elements occurs due to thermal conductivity, natural convection and radiation. In the natural air cooling mode, different designs of surfaces

(radiators) with different fin forms are used [3–5,9–13]. However, due to the small values of heat transfer coefficients 5–12 W/(m^{2}K) [3–5], a heat sink with natural convection is possible only at a relatively high temperature pressure and requires large heat transfer surface areas.

Forced air cooling, more efficient than natural cooling and simple to implement, greatly reduces the mass and dimensions of the equipment and, most importantly, increases the lifetime of the elements. In forced air cooling, the heat is transferred by forced convection and radiation. The values of the coefficients of heat transfer during forced convection of air are 70–170 W/(m^{2}K) [3–5]. The amount of heat removed during forced air cooling can be increased by the development of a heat-transfer surface, made in the form of radiators and other developed heat-exchange surfaces [14–18].

However, with diminishing sizes and increasing the specific of the heat flow of electronic components, the use of radiators of increased sizes leads to an increase in the temperature difference both in the contact area of the electronic component with the radiator and along the base of the radiator (Fig. 1a). The temperature and cooling efficiency are reduced. Expanding the possibility of air cooling of semiconductor elements of MED with high heat dissipation can be using two-phase heat transfer devices, in particular flat vapor chambers [19–21] and heat pipes [22–27]. They allow the local heat stream from the MED element to be efficiently dissipated to a larger heat transfer surface area of the heat pipe or the vapor chamber. If the vapor chamber is a ceramic [28] or silicon [29] flat heat pipe, then the semiconductor crystals of MED elements can be formed right on top of the ceramic heat pipe or vapor chamber. Compared with the traditional installation of cased elements on a heat pipe or vapor chamber, such technology eliminates the contact thermal resistance between the element casing and the vapor chamber, which reduces the temperature of the electronic component during operation and increases its reliability.

The most common types of heat pipes for cooling systems of MED are classical heat pipes [22], loop heat pipes [30,31], and loop thermosyphons [32–35]. Problem issues with the use of such cooling systems is the effective removal of heat from the condensation zone of a two-phase heat transfer device to the environment. As shown in [32], an increase in the intensity of heat transfer from the surface of a condenser of a loop heat pipe or thermosyphon leads to an increase in the efficiency of heat transfer in the cooling system and thus to a decrease in the temperature of the cooled element.

In order to reduce the thermal resistance of the air cooling system

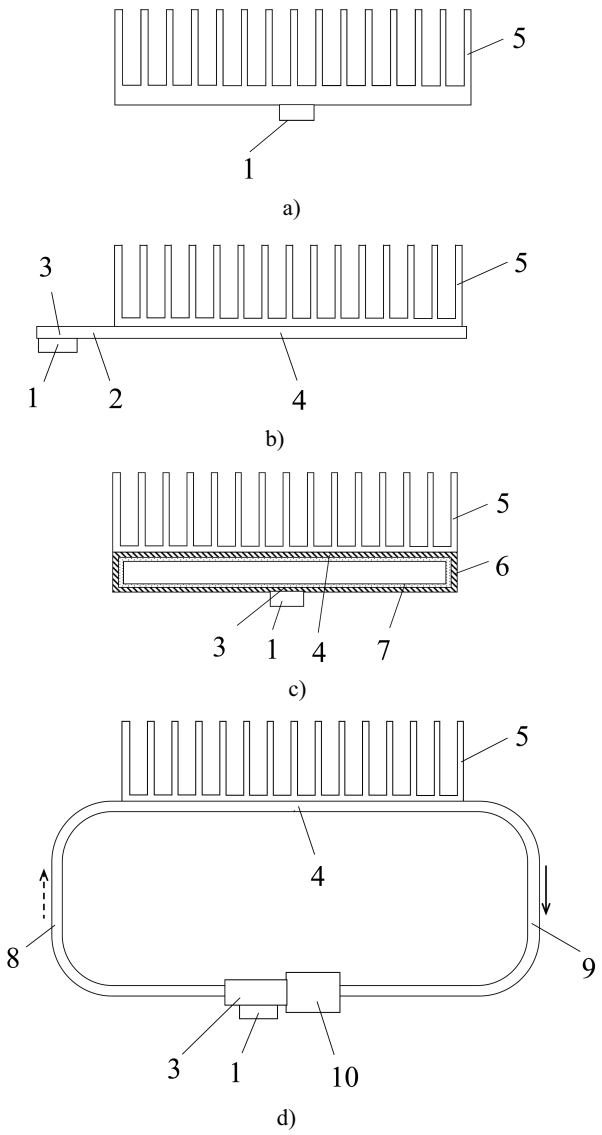

Figure 1: Schematic drawing of a cooling systems for a high-power electronic component using a radiator (a), radiator with a heat pipe (b), radiator with a vapor chamber (c), and radiator with a loop heat pipe (d): 1 – electronic component, 2 – heat pipe, 3 – evaporator, 4 – condenser, 5 – radiator, 6 – vapor chamber, 7 – wick, 8 – vapor line, 9 – liquid line, 10 – compensation chamber.

with a heat pipe or a vapor chamber, a radiator is installed on the outer surface of its body (Fig. 1b, c, and d). The heat removal efficiency can be improved, for example, by increasing the surface of the radiator. However, this leads to an increase in the size and mass of the radiator and the cooling system as a whole. For example, in [36] the radiator dimensions were 400×480×45 mm. Another option to increase the intensity of the heat transfer from the surface of the condenser of the loop heat pipe is to use more efficient heat transfer surfaces (radiators of a new design) installed for the condenser.

There are many studies on the development and research of various designs of radiators, heat exchangers and cooling channels. Thus, Baskova, Voropaiev [37] showed that a corrugation of the channel allows increasing the heat transfer up to 30% with an increase in the hydraulic resistance by 1.05 times in the range of Reynolds numbers from 2×10^3 to 1.4×10^4. In [38–40], finned lamellar radiators were studied, [17,38,39,41] dealt with needle-pin radiators. To study the heat transfer processes, aerodynamics and hydrodynamics, numerical simulation methods are widely used [42–49].

Computational fluid dynamics (CFD) modeling of a new type of radiator was carried out in [42]. It is shown that a sharp growth of heat transfer coefficient of the radiator can be achieved by making several conic or combined conic-cylindrical dead-end cavities with extra finning in the heat-transfer surface. It is determined that when the air velocity at the nozzle entrances is 50–100 m/s, the investigated designs of impact-jet radiators have a thermal resistance in the range of 0.5–2.2 °C/W. Huang *et al.* [43] proposed and studied numerically under natural convection conditions two novel models of fin heat sink, named the pin-plate fin heat sink (PPF) and the oblique-plate fin heat sink (OPF), by combining plate fins with pin fins and oblique fins. Heat transfer coefficients of PPF and OPF were higher by 12.6%–35.2% than those of three original models (plate fin, pin fin and oblique fin). In the paper of Royston Marlon *et al.* [44], heat sinks with different fin geometries (circular pin fin, triangle, ellipse, airfoil and reverse airfoil) were numerically analyzed using Ansys Fluent to determine their influence on thermal performance and airflow around the fins. The efficiency of the pin fins was found to be the highest and the airfoil fins with reverse orientation offers the minimum thermal resistance. In [45], the possible optimal thickness of a heat sink base was explored numerically with different convective heat transfer boundary conditions in a three

dimensional heat transfer model. Chen and Wang [46] proposed a novel trapezoid surface design applicable to an air-cooled heat sink under cross flow conditions. Based on the test results, it was found that either step or trapezoid design can provide a higher heat transfer conductance and a lower pressure drop at a specified frontal velocity. In study [47], a quick assessment of the performance and cost issue for rectangular fin and trapezoid fin was analytically investigated and experimentally verified.

Researchers at Igor Sikorsky Kyiv Polytechnic Institute have developed and tested a new heat transfer surface with lamellar-split finning for air-cooled systems [50,55,56,69]. The studies have shown that cutting the lamellar fins is an effective way to intensify the heat transfer and significantly reduce the operating temperature of the heat-charged MED element. At the same time, methods for computer simulation of such radiators are not being developed, which hinders their implementation into the practice of designing heat-loaded MEDs.

This study is aimed at developing a CFD modeling method for a new radiator design with lamellar-split fins, and verifying the data of the numerical experiment used in this research, in order to further optimize the geometric characteristics of the heat-dissipating finned surface of the cooling system and improving the MED performance in general.

2 Object, models and numerical simulation

2.1 Geometric model

Numerical study was performed using the finite element CFD models of heat transfer surfaces developed in the commercial ANSYS-Fluent software package.

The objects of the research were the basic design of the radiator with a smooth lamellar finning and two new modified designs of the same radiator: one with a lamellar-split finning and another with a lamellar-split finning with the petals rotated at a certain angle (Fig. 2). The results of numerical studies of the thermal and aerodynamic characteristics of the new radiator designs were compared with the same characteristics of the basic design and with the experimental data obtained earlier.

Three-dimensional motion and heat exchange of viscous fluid in the interfin semi-open channels of the lamellar-split finned surfaces (of all three designs) were calculated by constructing three CFD models with different fin designs. Geometric parameters of the surface did not change during

tests: the fins (height $h = 35$ mm, thickness $\delta = 0.55$ mm) were fixed perpendicular to the flat base (size $L \times L = 70 \times 70$ mm, thickness $b = 3$ mm) with a step of $t = 5$ mm. Copper was chosen as the material for the model.

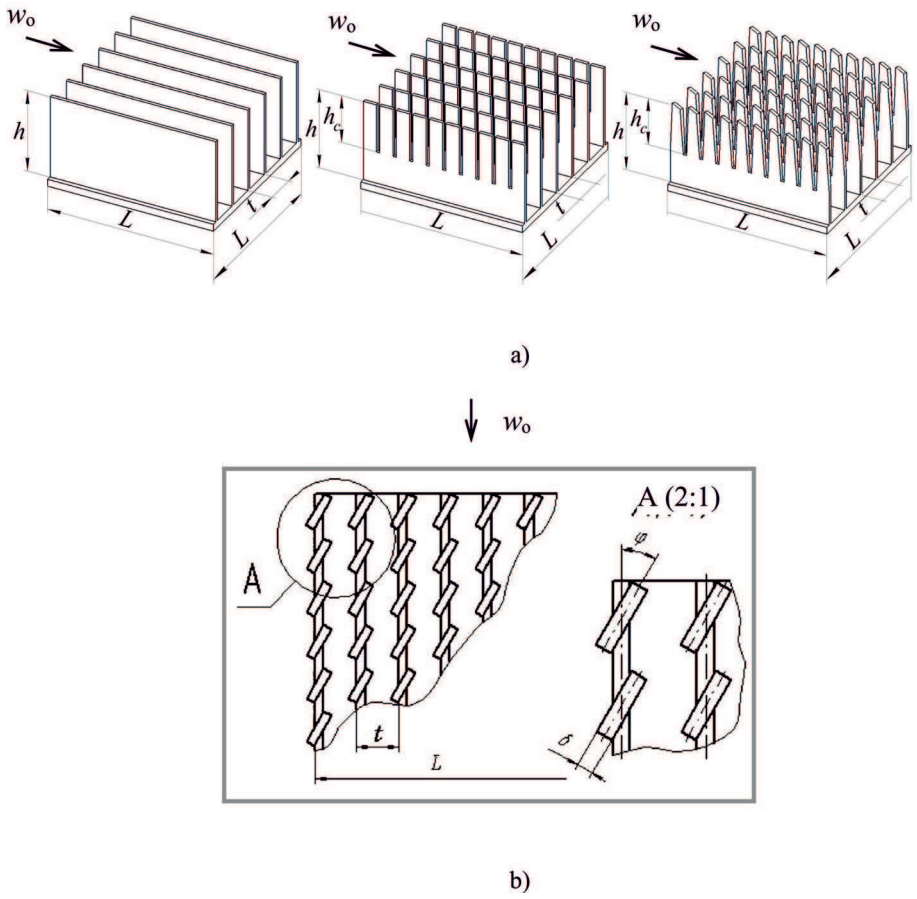

Figure 2: Schematic drawing of radiators (a) and top view (b) of the radiator model with lamellar-split finning and rotated petals.

First, a basic model with smooth lamellar fins was studied. Then the fins were split vertically, which transformed the surface into a system of so-called petals — separate rectangular parts of the fins. The cutting width (the distance between the petals) was selected in such a way that the total area of the heat-exchange surface of the split fin was not less than the surface area of the smooth non-split fin. The optimal depth of the cut was found to be $h_c/h = 0.6$. In the next experimental model, the petals were rotated at an angle of $\varphi = 30°$ against the direction of fluid flow (Fig. 2) [50]. The optimal value of the depth of the cut and the rotation angle of the 'petals' were chosen according to the experimental results of [50].

2.2 Calculated area and computational grid

When simulating this type of problem, even using modern high-performance computing programs, there are certain difficulties because the number of finite elements and the calculation time depend on the computing power of the personal computer and are thus limited. This is why in this study numerical calculations were performed only for one element of the heat-transfer surface.

Figure 3 shows the heat transfer surface located in the plane-parallel channel of the aerodynamic tube. The test element of the surface is drawn in thin lines and the arrows indicate the direction of the air flow w_o and the heat flux Q, which collectively determine the problem area.

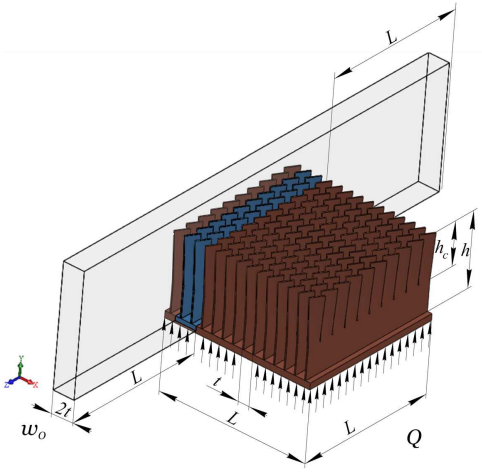

Figure 3: Problem area.

The development of the computational model was based on the geometric model of the calculated area. The discretization of the calculated area was carried out in accordance with the recommendations on how the characteristics of the finite elements grid affect the stability and convergence of the solution, and with the rules on the setting the boundary conditions. The calculated area was covered with an uneven tetrahedral grid with a minimum step of 0.1 mm becoming thicker toward the walls of the base and the fins of the heating element. An example of a three-dimensional computational grid for solid-state elements of the model is shown in Fig. 3.

To model the flow and heat exchange near the solid-state walls of the model, the Cartesian uneven grid was used, which is specified by the inflation function of the computation software. Figure 4a shows the calculation grid used to simulate the air flow in the interfin channels of the radiator. Figures 4b and Fig. 4c show an enlarged cross section of the experimental model of the area near the fin wall, which was modeled using the inflation function.

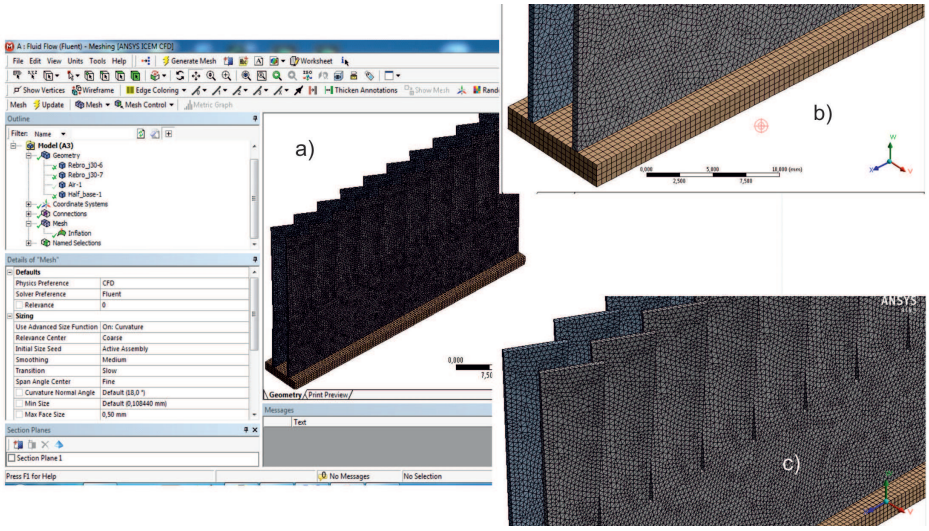

Figure 4: Computational grid for solid elements of the CFD model: the calculation grid used to simulate the air flow in the interfin channels of the radiator (a); a cross section of the experimental model of the area near the fin wall, which was modeled using the inflation function (b, c).

The inflation function is used to model adjacent layers that develop under the conditions of separating currents occurring on the surfaces of the initial sections of the interfin channels [51–54]. However, one must also take into

account that during the physical experiment, the heating surface is located in an aerodynamic tube [55,56], and for this reason it is also necessary to simulate the forming of the adjacent layer on the upper plane of the calculated area (Fig. 5).

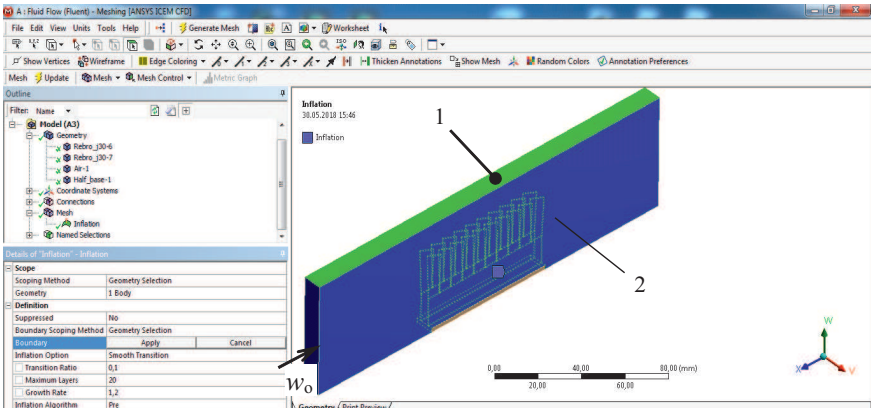

Figure 5: Visualization of the boundary conditions of the CFD model: 1 – upper wall of the aerodynamic tube, 2 – walls of the experimental increased surface.

Figure 5 shows all surfaces where the adjacent layer forms, which were taken into account when using the inflation function in accordance with the recommendations [57] as to the number of cells in the adjacent layer (20 in our case) and the size of the first cell 1×10^{-5} m, which satisfies the condition $y = \mathrm{Re}^{-1}$ in the wall normal direction. The Reynolds number was calculated using the velocity of the flow in the interfin channel, and the equivalent diameter was used as the characteristic size.

The absolute error of calculation of thermodynamic parameters, ultimately associated with the convergence and stability of the model, is chosen as discrepancy criterion of the model. The condition for the completion of the iterative calculation process was the achievement of a difference between the previous and subsequent values of thermodynamic parameters was 10^{-5}.

2.3 Coordinate system and boundary conditions

During the simulation, the same coordinate system was used as in experimental studies on surfaces: the positive direction of the OX axis corresponds to the longitudinal washing of the fin surface by air flow, the OY axis is directed along the side of the fin from the bottom of the channel,

and the positive direction of the OZ axis goes along the normal to the figure plane.

The planes (1) in Fig. 5 simulate solid (impenetrable) walls on which the adjacent layer develops. These are the upper and lower walls of the working area of the aerodynamic set up [55,56]. Inside the channel of this pipe, the experimental surface and the walls of the experimental increased surface were installed .

Preliminary simulation and calculations of heat exchange and aerodynamics of the expanded lamellar surfaces for cooling MED elements using various CFD models – shear stress transport (SST) model, renormalisation group (RNG) k-ε model, Reynolds stress model (RSM) – showed that the SST turbulence model is the most acceptable.

The model of turbulence SST (Menter's model) was chosen according to the results of comparison with other models of turbulence: RNG k-ε, RSM, not presented in this paper. The SST model was chosen due to the fact that it gives minimal discrepancies with the experimental data and well describes the problem with complex separated flows.

The algorithm chosen for implementing the model is based on an implicit finite-volume method for solving the Navier-Stokes equations closed by SST Menter's turbulence model, because the authors of the study [57,70–72] have shown that this model is the most suitable for calculating separating currents. The solution is initialized in the absolute coordinate system.

The thermophysical properties of air were set as polynomial temperature functions. The thermophysical properties of solids were fixed. The walls limiting the channel from above and from below were considered to be adiabatic.

The set task was formulated as a stationary problem and solved taking into account the requirement to keep the solution independent of the density of the computational grid.

On the lateral faces of the computational domain, the symmetric (symmetry) type of boundary conditions was chosen. A number of other authors, e.g., [73,74], also used the symmetric type of boundary conditions when modeling flows under forced convection in rectangular channels. In our studies, this type of boundary conditions was chosen due to the following consideration: since the pressure in all radiator channels is the same, then the boundary at the center of the interfin channel may be of a symmetrical nature when choosing a computational domain. It can be seen from the above figures that there are no overflows between the channels, which

confirms the validity of the choice of this type of boundary conditions.

The option of using periodic boundary conditions (periodic) was also considered. However, as a result of modeling with such boundary conditions, the calculated value of the temperature of the base of the finned surface (under a heat load of 100 W and blown by a current with a speed of 10 m/s) was 427 K, which contradicted the experimental results (348 K). Moreover, it was noted that the use of periodic boundary conditions requires a larger computational power, which is not always acceptable in design practice.

During simulation, the following boundary conditions were fixed for all standard sizes:

- the temperature of the oncoming stream near the heat transfer surface 289 K;
- the pressure drop between entering and leaving the working area, which corresponds to the average flow speed w_o = 11.6, 7.4, 4.6, 2.4 m/s;
- the heat power to be dissipated by the finned surface and evenly distributed along the base of the surface Q = 100, 80, 60, 40 W (Fig. 3).

2.4 Data processing method

The experimental data for all CFD models were processed using a general technique, according to which the commercial CFD software package was used to determine the area of the channel before entering into the calculation model, F_{ch}^{in}, the speed, w_o, and the temperature, T_o, of the oncoming stream (set according to the boundary conditions), the cross-sectional area of the interfin channel, F_{ch}, the flow rate in the interfin channel, the pressure drop across the ribbed surface, ΔP, the average surface temperature of the fin, T_{as} and the basis temperature, T_b, and the heat flux density q dissipated by the fin surface. After calculating these data, the average surface convective heat transfer coefficient was calculated using the following dependence:

$$\alpha_c = q/(T_{as} - T_o) \; . \tag{1}$$

To determine the fin efficiency, E, of a flat rectangular fin that is mounted on a flat base, we can use the formula given in [59] (in our case, the relative length of the line of contact between the fin l_{cfin} and the base L is 1,

$L_c = l_{cfin}/L = 1$).

When calculating the Nusselt and Reynolds numbers, an equivalent diameter, d_e, of the flow cross-section of the surface was used as the characteristic length and calculated by the formula

$$d_e = 4F_{ch}/P = 4[(t-\delta)h + t(58-h)]/(2h+t)\ , \tag{2}$$

where F_{ch} is the area of the flow cross-section at a step t, P is the wetted perimeter (Fig. 6).

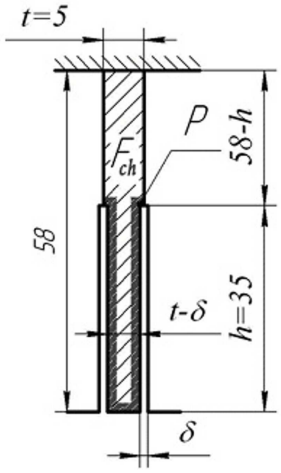

Figure 6: Schematic drawing for calculating the equivalent diameter of the finned surface.

Study of the convective heat transfer laws for heat exchange surfaces was reduced to determining the dependence of the dimensionless Nusselt numbers on the average surface convective heat transfer coefficients, on the Reynolds number, as well as determining average values of heat exchange coefficient along the surface. The velocity of the oncoming flow, w_o, was taken as the characteristic air velocity. The thermal conductivity coefficient, λ, and kinematic viscosity coefficient, ν, that are necessary to calculate the Nusselt and Reynolds numbers were determined using the average balance temperature of air by means of commercial CFD solver.

The studies were conducted under conditions of forced convection, the range of Reynolds number was $2.5\times10^3 < \mathrm{Re} < 11\times10^3$, which corresponds to the transitional flow regime.

3 Analysis of the results of numerical studies

The flow channel visualization is shown in Fig. 7. The visualization plane is selected at a distance of 5 mm from the top edges of the 'petals'. Figure 7a shows the air flow in the channel between adjacent fins. As can be seen from this figure , there is no observable air overflow in the space between the fins. Figure 7b shows the visualization of the flow displaying the surfaces of the 'petals', while Fig. 7c shows the same, but without the surface of the 'petals' (only contours are shown). Swirls of the air flow are shown in darker blue. As can be seen from the above figures, there is no observable effect of zeroing and overflow from the cut fin with segment rotation into adjacent channels.

The results of numerical studies were presented as dependences of the Nusselt number, Nu, and Euler number, Eu, on the Reynolds number.

The obtained results were compared with the calculations of the average surface heat transfer using the formulas recommended in [55]:

$$\mathrm{Nu}_c = 0.1485\,\psi^{-0.3}\,C_F\,(L/d_e)^{-0.13}\,\mathrm{Re}^{0.75}\,, \tag{3}$$

where ψ is the finning coefficient. The coefficient C_F accounts for the influence of the relative splitting depth, h_c/h, and the rotation angle, φ, of the petals, and is determined by the function

$$C_F = \frac{1}{F_1\,e^{\frac{h_c}{h}} - F_2\,\frac{h_c}{h}}\,, \tag{4}$$

where the coefficients F_1 and F_2 account for the influence of the rotation angle of the petals and are determined by the following dependencies:

$$F_1 = \sqrt{\frac{2.7}{e^{\varphi}} - 1.66\,e^{\varphi} + 4.25\,\varphi}\,, \tag{5}$$

$$F_2 = \ln\left(-\frac{8.5}{e^{\varphi}} - 4.7\,\varphi + 14.3\right)\,. \tag{6}$$

Comparative analysis of the aerodynamic resistance was also performed using the dependence recommended in [56]:

$$\mathrm{Eu} = 34\left(\frac{H}{F}\right)^{-0.47} e^{\ln\left(\frac{1.36}{e^{\varphi}}+3.8\right)\frac{h_p}{h}}\,\mathrm{Re}^{-\left[0.74\left(\frac{H}{F}\right)^{-0.26}\right]}\,, \tag{7}$$

where H/F is a generalization parameter that accounts for the geometry of the increased surfaces and is defined as the ratio of the total area of the studied surface, H, to the area of the flow ('live') section, F.

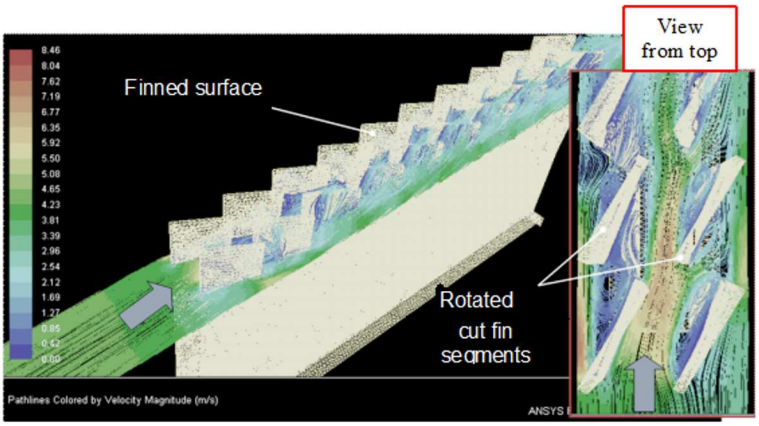

(a)

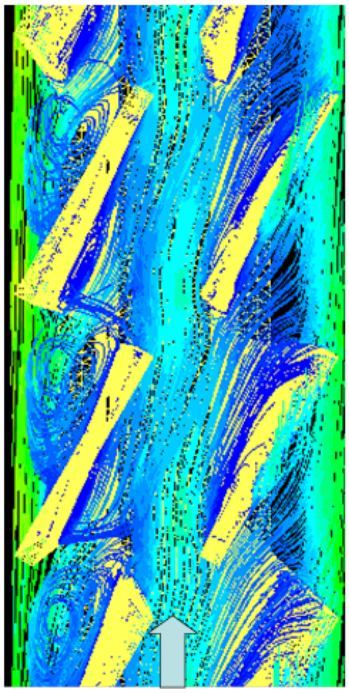

(b)

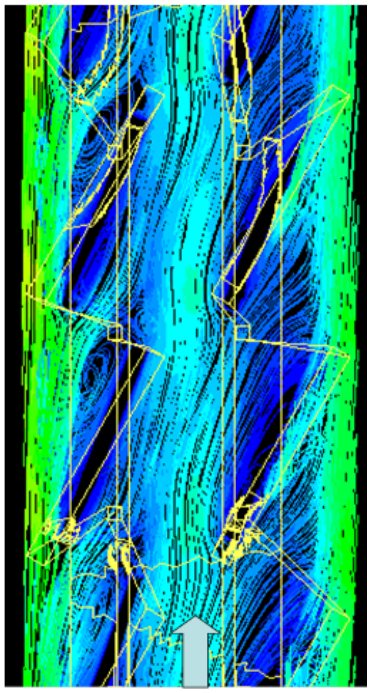

c)

Figure 7: Visualization of the flow in the channel: (a) general view, (b) view on an enlarged scale with the surfaces of the 'petals' displayed, (c) – the same without specifying the surface of the 'petals' (only contours are shown).

The results of the heat exchange simulation for the tested surfaces are presented for the Reynolds number range $2.5 \times 10^3 < \mathrm{Re} < 11 \times 10^3$, within the thermal capacities $Q = 40, \ldots, 100$ W at a temperature of the cooling air at the surface 289 K (Fig. 8a).

The analysis of the calculated data obtained from a physical experiment shows that cutting the fins and rotating the petals relative to the oncoming stream increases the heat transfer intensity. According to Fig. 8, the surface with uncut lamellar fins ($h_c/h = 0$) has the lowest level of convective heat transfer. The split fins ($h_c/h = 0.6$) have a 14–15% higher level of convective heat transfer intensity.

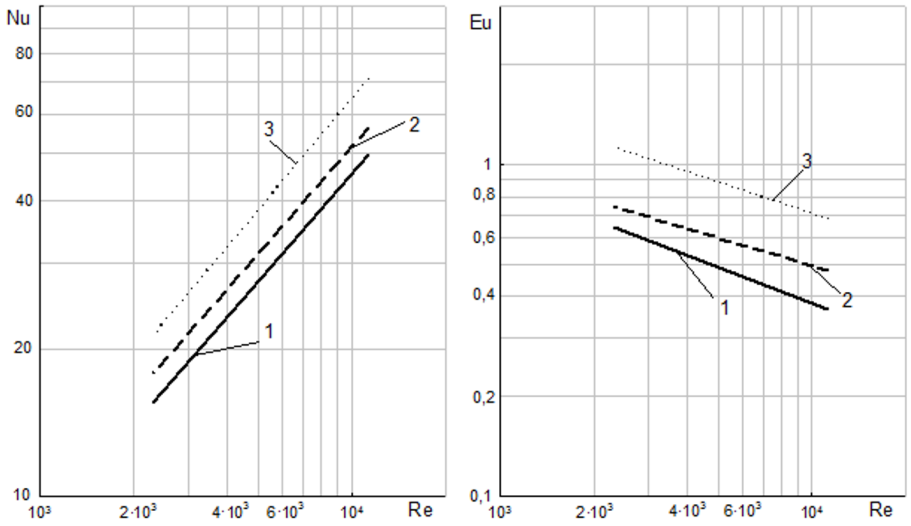

(a) b)

Figure 8: Results of heat exchange (a) and aerodynamic resistance (b) simulation: 1 – surface with uncut fins, 2 – $h_c/h = 0.6$, 3 – $h_c/h = 0.6$, and $\varphi = 30°$.

Rotating the petals leads to an even bigger increase in the heat transfer intensity. The analysis of the calculated data obtained from a physical experiment showed that when the petals are rotated at an angle of 30°, the heat transfer intensifies by 24–25% compared to the split ($h_c/h = 0.6$) surface without petal rotation, and by 39–42% compared to the smooth lamellar-finned surface ($h_c/h = 0$).

The increase in heat transfer coefficient in the design with cut fins and rotated 'petals' can be explained by destruction and disruption of the boundary layers in the gaps between the cut segments of the fins, separation

of the boundary layers on the front edges of the 'petals' and turbulization of the flow in the interfin sections of the surface.

The results on aerodynamic resistance simulation are presented in Fig. 8b. Analyzing the data in the figure, one can see that the surface with smooth lamellar fins has the smallest aerodynamic drag. Making cuts to the depth of $h_c/h = 0.6$ increases the drag, compared to the uncut surface, by an average of 20–28%. The increase in aerodynamic drag is most likely caused by the tear vortices that appear at the cut edges of the fins, which increase the drag of the radiator.

Rotating the petals at an angle of 30° relative to the oncoming flow leads to blocking of the flow area of the channel with the turned 'petals' of the split parts of the ribs, and to further increase in the aerodynamic drag. Thus, the cut surfaces with rotated petals have a 40–55% greater aerodynamic drag than the surfaces without petal rotation, and an 80–85% increase in aerodynamic drag compared with the smooth fins.

In order to obtain more complete information on the verification of the CFD model, numerical data were compared with the results of calculations by formulas (3) and (7).

Analysis of data in Fig. 9 indicates that the used Menter's turbulence model does not quite accurately predict the flow inside the interfin channel created between solid lamellar fins. Further experiments prove that it is better to use the Launder-Spalding model for a channel formed by smooth solid fins. However, these models can not predict the tearing currents [51–54], which appear in the cut fins when the sections are rotated against the oncoming flow.

Figures 10 and 11 show the verification results on the average heat transfer and aerodynamic drag of the surfaces with split fins and rotated sections. As shown in the figures, the difference between the CFD simulation data and the calculated results obtained from a physical experiment is 23%. The observed discrepancies between the model and the experiment depend on many factors, one of which may be the inaccuracy of the experimental data used as the basis for the numerical problem, and this could ultimately lead to an error in model solving. This value is acceptable in computing practice and indicates that the developed CFD model is an efficient one, and the methods used to construct the CFD model can also be used for more complex tasks.

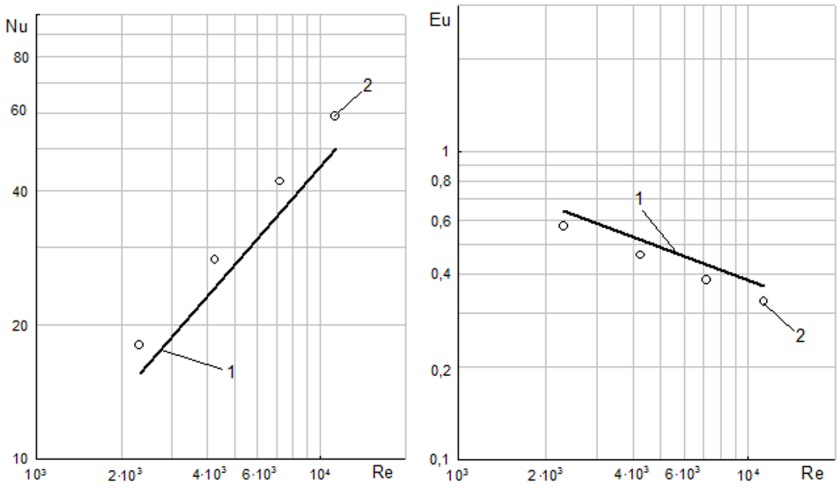

(a) b)

Figure 9: Verification of simulation results of heat transfer (a) and aerodynamic resistance (b) of the surface with smooth lamellar fins washed by the air flow: 1 – CFD modeling data, 2 – calculation by the formulas (3) [55] and (7) [56] on the basis of experimental data.

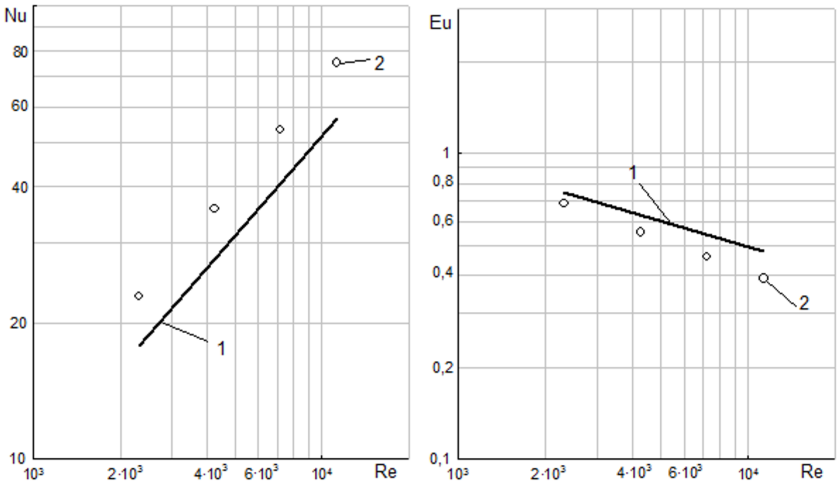

(a) b)

Figure 10: Verification of simulation results of heat transfer (a) and aerodynamic resistance (b) of the surface with split fins with $h_c/h = 0.6$ and $\varphi = 0^\circ$ washed by the air flow: 1 – CFD modeling data, 2 – calculation by the formulas (3) [55] and (7) [56] on the basis of experimental data.

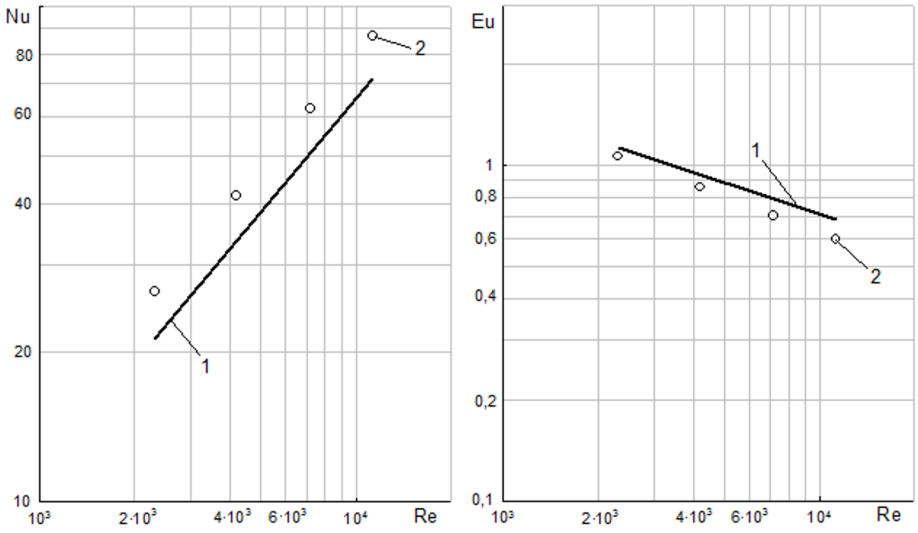

(a) b)

Figure 11: Verification of simulation results of heat transfer (a) and aerodynamic resistance (b) of the surface with split fins $h_c/h = 0.6$ and rotated petals washed by the air flowand $\varphi = 0°$: 1 – CFD modeling data, 2 – calculation by the formulas (3) [55] and (7) [56] on the basis of experimental data.

4 Conclusions

Preliminary calculations of heat exchange and aerodynamics of the expanded lamellar surfaces for cooling MED elements using various CFD models (SST, RNG k-ε, RSM) allow concluding that the SST turbulence model (Menter's model) is the most acceptable.

The analysis of the calculation using the developed CFD model shows that having the finite parts of the fins cut into separate 'petals' allows increasing the heat transfer intensity by 15% while simultaneously increasing the aerodynamic drag by 20%, as compared to the lamellar radiator. Cutting the finite edges of the fins into individual 'petals' and rotating those petals by an angle of 30° relative to the flow leads to an increase in the heat transfer intensity by 45% while simultaneously increasing the aerodynamic drag by 80–85%.

The increase in heat transfer coefficient in the design with cut fins and rotated 'petals' can be explained by destruction and disruption of the boundary layers in the gaps between the cut segments of the fins, separation

of the boundary layers on the front edges of the 'petal' and turbulization of the flow in the interfin sections of the surface.

The increase in the aerodynamic resistance of the radiator with the rotated 'petals' of the cut fins is most likely caused by the tearing vortices that appear at the cut edges of the fins, and the blockage of the flow area of the channel with the rotated 'petals' of the cut fins.

The numerical method proposed is aimed at improving air cooling systems during thermophysical design of electronic devices by using highly effective finned surfaces.

The authors have developed a heat exchange and aerodynamic resistance CFD model for a radiator with lamellar-split fins, which can be used in air cooling systems for various electronic devices. In particular, the obtained results can be useful in the cooling systems of central processor devices and other powerful electronic components [60,61], power amplifiers for transmitting modules of radar systems [62], promising energy-saving solid-state light sources [63–66], and rocket and space electronics devices [67,68].

Received 8 December 2018

References

[1] Bogatin E.: *Chip packaging: Thermal requirements and constraints*. In: Roadmaps of Packaging Technology (D. Potter and L. Peters, Eds.), (Chap. 6). Integrated Circuit Engineering Corporation, 1997, 6-1–6-32. http://smithsonianchips.si.edu/ice/cd/PKG_BK/CHAPT_06.PDF

[2] Lin Wei-Keng.: *Theoretical derivation of junction temperature of package chip*, In: Electronics Cooling, Chap. 8, (S.M. Sohel Murshed, Ed.),. 2016, 151–171.

[3] Chernyshev A.A.: *Fundamentals of Reliability of Semiconductor Devices and Integrated Circuits*. Radio i Svyaz, Moscow 1988 (in Russian).

[4] Rotkop L.L., Spokoynyy Yu.Ye.: *Thermal Management in the Design of Radioelectronic*. Sovetskoye Radio, Moscow 1976 (in Russian).

[5] Dul'nev G.N.: *Heat and mass transfer in radioelectronic equipment*. In: Design and Production of Radio Equipment. Vysshaya Shkola, Moscow 1984 (in Russian).

[6] Wei J.: *Challenges in cooling design of CPU packages for high-performance servers*. Heat Transfer Eng. **29**(2008), 2, 178–187, https://doi.org/10.1080/01457630701686727

[7] Nakayama W.: *Heat in computers: Applied heat transfer in information technology*. J. Heat Trans.-T ASME **136**(2014), 1, 013001-1–013001-22. https://doi.org/10.1115/1.4025377

[8] Sullivan O., Alexandrov B., Mukhopadhyay S., Kumar S.: *3D compact model of packaged thermoelectric coolers*. J. Electron. Packaging **135**(2013), 3, 031006-1–031006-7, https://doi.org/10.1115/1.4024653

[9] Jubear A.J., Al-Hamadani Ali A.F.: *The effect of fin height on free convection heat transfer from rectangular fin array*. Int. J. Recent Sci. Res. (IJRSR) **6**(2015), 7, 5318–5323, https://www.researchgate.net/publication/280933185

[10] Jubear A.J.: *An experimental investigation of heat transfer enhancement for vertical interrupted fin in free convection*. Int. J. Recent Sci. Res. (IJRSR) **8**(2017), 6, 17279–17284, http://dx.doi.org/10.24327/ijrsr.2017.0806.0321

[11] Goshayeshi H.R, Ampofo F.: *Heat transfer by natural convection from a vertical and horizontal surfaces using vertical fins*. Energy Power Eng. (EPE) **1**(2009), 2, 85–89. http://dx.doi.org/10.4236/epe.2009.12013

[12] Haghighi S.S., Goshayeshi H.R., Safaei Mohammad Reza: *Natural convection heat transfer enhancement in new designs of plate-fin based heat sinks*. Int. J. Heat Mass Tran. **125**(2018), 640–647. https://doi.org/10.1016/j.ijheatmasstransfer.2018.04.122

[13] Pismennyi Ye.N., Rogachev V.A., Bosaya N.V.: *Investigation into efficiency characteristics of a new heat transfer surface with mesh finning under free convection*. Heat Transf. Res. **30**(1999), 1, 30–35.

[14] Chen CH., Wang C.-C.: *A novel trapezoid fin pattern applicable for air-cooled heat sink*. Heat Mass Transfer **51**(2015), 11, 1631–1637, https://doi.org/10.1007/s00231-015-1666-4

[15] Chingulpitak S., Chimres N., Nilpueng K., Wongwises S.: *Experimental and numerical investigations of heat transfer and flow characteristics of cross-cut heat sinks*. Int. J. Heat Mass Tran. **102**(2016), 142–153, https://doi.org/10.1016/j.ijheatmasstransfer.2016.05.098

[16] Teerstra P., Yovanovich M.M., Culham J.R.: *Analytical forced convection modeling of plate fin heat sinks*. J. Electron. Manuf. **10**(2000), 4, 253–261, https://doi.org/10.1109/STHERM.1999.762426

[17] Yu X., Feng J., Feng Q., Wang Q.: *Development of a plate-pin fin heat sink and its performance comparisons with a plate fin heat sink*. Appl. Therm. Eng. **25**(2005), 1-2, 173–182. https://doi.org/10.1016/j.applthermaleng.2004.06.016

[18] Shih C.J., Liu G.C.: *Optimal design methodology of plate-fin heat sinks for electronic cooling using entropy generation strategy*. IEEE T COMP PACK T **27**(2004), 3, 551–559, https://doi.org/10.1109/TCAPT.2004.831812

[19] Bulut M., Kandlikar S.G., Sozbir N.: *A review of vapor chambers*. Heat Transfer Eng. **40**(2019), 19, 1551–1573 , https://doi.org/10.1080/01457632.2018.1480868

[20] Reyes M., Alonso D., Arias J.R., Velazquez A.: *Experimental and theoretical study of a vapour chamber based heat spreader for avionics applications*. Appl. Therm. Eng. **37**(2012), 51–59, http://dx.doi.org/10.1016/j.applthermaleng.2011.12.050

[21] Wang J.-C., Wang R.-T., Chang T.-L., Hwang D.S.: *Development of 30 Watt high-power LEDs vapor chamber-based plate*. Int. J. Heat Mass Tran. **53**(2010), 19-20, 3990–4001, http://dx.doi.org/10.1016/j.ijheatmasstransfer.2010.05.018

[22] Reay D.A., Kew P.A., McGlen R.J.: *Heat Pipe: Theory, Design and Applications* (6th Edn.) Buterworth-Heinemann Amsterdam 2014.

[23] Vasil'ev L.L. Jr, Grakovich L.P., Dragun L.A., Zhuravlev A.S., Olekhnovich V.A., Rabetskii M.I.: *System for cooling of electronic components.* J. Eng. Phys. Thermophys. **90**(2017), 1, 95–101, http://dx.doi.org/10.1007/s10891-017-1543-8

[24] Mochizuki M., Nguyen T., Mashiko K., Saito Y., Nguyen T., Wuttijumnong V.: *A review of heat pipe application including new opportunities.* Front. Heat Pipes **2**(2011), 013001. https://doi.org/10.5098/fhp.v2.1.3001

[25] Nikolaienko Yu.E.: *Schematics of the architecture of heat rejection from functional modules of a computer with the help of two-phase heat-transfer devices.* Upravlyayushchie Sistemy i Mashiny **2**(2005), 29–36, http://ela.kpi.ua/handle/123456789/16362 URL:http://www.scopus.com/inward/record.url?eid=2-s2.0-33644653599&partnerID=MN8TOARS

[26] Faghri A.: *Heat pipes: Review, opportunities and challenges.* Front. Heat Pipes **5**(2014), 1-48. http://dx.doi.org/10.5098/fhp.5.1

[27] Kravets V.Yu., Nikolaenko Yu.E., Nekrashevich Ya.V.: *Experimental studies of heat-transfer characteristics of miniaturized heat pipes.* Heat Transf. Res. **38**(2007), 6, 553–563, http://dx.doi.org/10.1615/HeatTransRes.v38.i6.70

[28] Nikolaenko Yu.E., Rotner S.M.: *Using laser radiation for the formation of capillary structure in flat ceramic heat pipes.* Tech. Phys. Lett. **38**(2012), 12, 1056–1058. http://dx.doi.org/10.1134/S1063785012120085 http:// www.scopus.com/inward/record.url?eid=2-s2.0-84872154463&partnerID=MN8TOARS

[29] Cai1 Q., Chen B.C, Tsai C.: *Design, development and tests of high-performance silicon vapor chamber.* J. Micromech. Microeng. **22**(2012), 035009, 1-9. http://dx.doi.org/10.1088/0960-1317/22/3/035009

[30] Pastukhov V.G., Maidanik Yu.F., Vershinin C.V., Korukov M.A.: *Miniature loop heat pipes for electronics cooling.* Appl. Therm. Eng. **23**(2003), 1125–1135. http://dx.doi.org/10.1016/S1359-4311(03)00046-2

[31] Mikielewicz D., Błauciak K.: *Investigation of the influence of capillary effect on operation of the loop heat pipe.* Arch. Thermodyn. **35**(2014), 3, 59–80. http://dx.doi.org/10.2478/aoter-2014-0021

[32] Kiseev V., Sazhin O.: *Heat transfer enhancement in a loop thermosyphon using nanoparticles/water nanofluid.* Int. J. Heat Mass Tran. **132**(2019), 557–564. https://doi.org/10.1016/j.ijheatmasstransfer.2018.11.109

[33] Bieliński H., Mikielewicz J.: *Computer cooling using a two phase minichannel thermosyphon loop heated from horizontal and vertical sides and cooled from vertical side.* Arch. Thermodyn. **31**(2010), 4, 51–59. http://dx.doi.org/10.2478/v10173-010-0027-4

[34] Bielinski H., Mikielewicz J.: *Application of a two-phase thermosyphon loop with minichannels and a minipump in computer cooling.* Arch. Thermodyn. **37**(2016), 1, 3–16, http://dx.doi.org/10.1515/aoter-2016-0001

[35] Vasiliev L., Grakovich L.,.Rabetsky M., Zhuravlyov A., Vassiliev JR L.: *Flat polymer loop thermosyphons*. Arch. Thermodyn. **39**(2018), 1, 75–90. http://dx.doi.org/10.1515/aoter-2018-0004

[36] Nemec P., Malcho M..: *Influence of the ambient temperature on the cooling efficiency of the high performance cooling device with thermosiphon effect*. EPJ Web Conf. **180**(2018), 02073 , 1–4. https://doi.org/10.1051/epjconf/201818002073

[37] Baskova O., Voropaiev G.: *Investigation of flow structure and heat exchange formation in corrugatedpipes at transient Reynolds numbers*. East. Eur. J. Enterp. Technol. **3**(2017), 8(87), 40–45, http://dx.doi.org/10.15587/1729-4061.2017.103880

[38] Chernyshev A.A., Ivanov V.I., Aksenov A.I., Glushkova D.N.: *Thermal management of electronic devicess*. Energiya. Moscow 1980 (in Russian).

[39] Jonsson H., Moshfegh B.: *Modeling of the thermal and hydraulic performance of plate fin, strip fin, and pin fin heat sinks — Influence of flow bypass*. IEEE T. Comp. Pack. T. **24**(2001), 2, 142–149. http://dx.doi.org/10.1109/6144.926376

[40] El-Sayed S.A., Mohamed S.M., Abdel-latif A.M., Abouda A.-H. E.: *Investigation of turbulent heat transfer and in longitudinal rectangular-fin arrays of d geometries and shrouded fin array*. Exp. Therm. Fluid Sci. **26**(2002), 8, 879–900, http://dx.doi.org/10.1016/S0894-1777(02)00159-0

[41] Kim K.-Y., Moon M.-A.: *Optimization of a stepped circular pin-fin array to enhance heat transfer performance*. Heat Mass Transfer **46**(2009), 63–74. https://doi.org/10.1007/s00231-009-0544-3

[42] Trofimov V.E., Pavlov A.L., Storozhuk A.S.: *CFD-simulation of impact jet radiator for thermal testing of microprocessors*. Tekhnologiya i Konstruirovanie v Elektronnoi Apparature (2018), 5-6, 30–36, http://dx.doi.org/10.15222/TKEA2018.5-6.30 (in Russian).

[43] Yicang Huang, Shengnan Shen, Hui Li, Yunjie Gu.: *Improved thermal design of fin heat sink for high-power LED lamp cooling*. In: Proc. 17th Int. Conf Electronic Packaging Technology (ICEPT) IEEE, 2016, 1069–1074, https://doi.org/10.1109/ICEPT.2016.7583311

[44] Mendonca Royston Marlon, Yalamarty Sai Sharan, Kini Chandrakant R.: *Numerical analysis of heat sink for LED lighting modules*. Int. J. Res. Eng. Technol. (IJRET) **4**(2015), 03, 142–150. https://doi.org/ 10.15623/ijret.2015.0403025

[45] Li J., Shi Z.-S.: *3D numerical optimization of a heat sink base for electronics cooling*. Int. Commun. Heat Mass **39**(2012), 2, 204–208. https://doi.org/10.1016/j.icheatmasstransfer.2011.12.001

[46] Chen, C.-H., Wang, C.-C.: *A novel trapezoid fin pattern applicable for air-cooled heat sink*. Heat Mass Transfer **51**(2015), 11, 1631–1637, https://doi.org/10.1007/s00231-015-1666-4

[47] Chen H.-L., Wang C.-C.: *Analytical analysis and experimental verification of trapezoidal fin for assessment of heat sink performance and material saving*. Appl. Therm. Eng. **98**(2016), 203–212, http://dx.doi.org/10.1016/j.applthermaleng.2015.11.131

[48] Voropaev G.A., Dimitrieva N.F.: *Simulation of the turbulent-energy redistribution in a diluted polymer solution*. J. Eng. Phys. Thermophys. **86**(2013), 1, 131–144. https://doi.org/10.1007/s10891-013-0813-3

[49] Voropayev G.A., Rozumnyuk N.V.: *Numerical simulation of turbulent flows over compliant surfaces*. Int. J. Fluid Mech. Res. **30**(2003), 1, 91–108, https://doi.org/10.1615/InterJFluidMechRes.v30.i1.9

[50] Pismennyi E.N., Terekh A.M., Rogachev V.A., Burlei V.D., Rudenko A.I.: *Calculation of convective heat transfer of plane surfaces with wire-net finning immersed in a cross-flow*. Heat Transfer Research **36** (2005), 1-2, 39–46. https://doi.org/10.1615/HeatTransRes.v36.i12.60

[51] Legkii V.M., Rogachev V.A.: *Local heat transfer on the entrance segment of a tube with a sharp inlet edge. 2. Correction for the entrance segment under turbulent boundary layer conditions*. J. Eng. Phys. Thermophys. **65**(1993), 2, 722–725, https://doi.org/10.1007/BF00861532

[52] Legkii V.M., Rogachev V.A.: *Local heat transfer on the entrance segment of a tube with a sharp inlet edge. 1. Nature and behavior of heat transfer intensity extrema*. J. Eng. Phys. Thermophys. **65**(1993), 2, 715–721. https://doi.org/10.1007/BF00861531

[53] Legkij V.M., Rogachev V.A.: *Local heat exchange in the starting segment of a pipe with a sharp front edge. 1. The nature and behaviour of heat exchange intensity extremums*. Inzhenerno-Fizicheskii Zhurnal **65**(1993), 2, 131–138 (in Russian).

[54] Legkij V.M., Rogachev V.A.: *Local heat exchange in the starting segment of a pipe with a sharp front edge. 2. Allowing for the starting segment under the turbulent flow conditions in the boundary layer*. Inzhenerno-Fizicheskii Zhurnal, **65**(1993), 2, 139–143, (in Russian).

[55] Pismenniy Ye.N., Burley V.D., Terekh A.M., Baranyuk A.V., Tsvyashchenko Ye.V.: *Heat transfer of flat lamellar surfaces with split finning under forced convection*. Promyshlennaya teplotekhnika **27**(2005), 4, 11–16 (in Russian).

[56] Pismenniy Ye.N., Terekh A.M., Rogachov V.A., Burley V.D., Baranyuk A.V.: *Aerodynamic resistance of lamellar surfaces with split fins in forced convection*. Promyshlennaya teplotekhnika **28**(2006), 4, 29–33 (in Russian).

[57] Bystrov Yu.A., Isayev S.A., Kudryavtsev N.A., Leont'yev A.I.: *Numerical Simulation of Vortex Intensification of Heat Exchange in Tube Stacks*. St. Petersburg: Sudostroyeniye 2005.

[58] Tang Y., Lin L., Zhang S., Zeng J., Tang K., Chen G., Yuan W.: *Thermal management of high-power LEDs based on integrated heat sink with vapor chamber*. Energ. Convers. Manage. **151**(2017), 1–10. http://dx.doi.org/10.1016/j.enconman.2017.08.087

[59] Pismennyi E.N., Bagrii P.I., Terekh A.M., Semenyako A.V.: *Optimization of the ribbing of a new heat exchange surface of flat-oval tubes*. J. Eng. Phys. Thermophys. **86**(2013), 5, 1066–1071. https://doi.org/10.1007/s10891-013-0929-5

[60] Naphon P.: *CPU cooling by vapor chamber with R-141b as working fluid*. Asian J. Eng. Technol. **02**(2014), 2, 161–167.

[61] Smitka M., Malcho M., Nemec P., Kolkova Z.: *Use of LHP for cooling power electronic components*. EPJ Web Conf. **45**(2013), 01046-1– 01046-4. http://dx.doi.org/10.1051/epjconf/20134501046

[62] Te Riele G,J., Wits W.W.: *Heat pipe array for planar cooling of rotating radar systems*. Joint Conf. 19th IHPC and 13th IHPS, Pisa, June 10-14, 2018, 1–8. https://www.researchgate.net/publication/326587888_Heat_pipe_array_for_-planar_cooling_of_rotating_radar_systems

[63] Wang J.-C., Wang R.-T., Chang T.-L., Hwang D.-S.: *Development of 30 Watt high-power LEDs vapor chamber-based plate*. Int. J. Heat Mass Tran. **53**(2010), 19-20, 3990–4001, http://dx.doi.org/10.1016/j.ijheatmasstransfer.2010.05.01

[64] Nikolaenko Yu.E., Kravets V.Yu., Naumova A.N., Baranyuk A.V.: *Development of the ways to increase the lighting energy efficiency of living space*. Int. J. Energ. Clean Env. **18**(2017), 3, 275–285. https://doi.org/10.1615/InterJEnerCleanEnv.2018021641

[65] Jong-Soo K., Jae-Young B., Eun-Pil K.: *Analysis of the experimental cooling performance of a high-power light-emitting diode package with a modified crevice-type vapor chamber heat pipe*. J. Korean Soc. Marine Eng. **39**(2015), 8, 801–806. http://dx.doi.org/10.5916/jkosme.2015.39.8.801

[66] Nikolaenko T.Yu., Nikolaenko Yu.E.: *New circuit solutions for the thermal design of chandeliers with light emitting diodes*. Light Eng. **23**(2015), 3, 85–88. http://www.scopus.com/inward/record.url?eid=2-s2.0-84966507707&partnerID=MN8TOARS

[67] Prisniakov K., Marchenko O., Melikaev Yu., Kravetz V., Nikolaenko Yu., Prisniakov V.: *About the complex influence of vibrations and gravitational fields on serviceability of heat pipes in composition of the space-rocket systems*. Acta Astronaut. **55**(2004), 3-9, 509–518, http://dx.doi.org/10.1016/j.actaastro.2004.05.005.

[68] Marchenko O., Prisniakov K., Prisniakov V., Kravez V., Nikolaenko Yu.: *Influence of Non-Stationary Conditions on Reliability of Space Systems with Heat Pipes under the Effect of Vibrations*. In Proc. 55th Int. Astronautical Cong. IAF, IAA, IISL, Vancouver, Oct. 4-8, 2004, **4**(2004), 2301–2311, http://dx.doi.org/10.2514/6.IAC-04-I.P.04

[69] Pysmennyy Ye.M., Epik E. Ya., Terekh O.M., Rudenko O.I., Baranyuk O.V.: *Peculiarities of the flow on the flat split rfins of cooling elements of the radio electronic equipment*. Res. Bull. National Technical University of Ukraine Igor Sikorsky Kyiv Politechnic Institute 3(53) 2007 (in Ukrainian).

[70] Li Z., Huai X., Tao Y., Chen H.: *Effect of thermal property variations on the liquid flow and heat transfer in microchanel heat sinks*. Appl. Therm. Eng. **27**(2007), 17–18, 2803–2814, https://doi.org/10.1016/j.applthermaleng.2007.02.007

[71] Diyev M.D., Kolesnikova A.A.: *Numerical simulation of intensification of turbulent heat exchange in a rectangular channel using Fluent CFD package*. In: Problems of gas dynamics and heat and mass transfer in power plants; Vol. 2. Proc. XVI School-Seminar of Young Scientists and Specialists, St. Petersburg 2007, 362–365 (in Russian).

[72] Frost U., Moulden T., Eds.: *Turbulence. Principles and Applications*. Mir, Moscow 1980.

[73] Jaffal H.M., Jebur H.S., Hussein A.A.: *Numerical and experimental investigations on the performance characteristics for different shapes pin fin heat sink*. IJOCAAS **4**(2018), 3, 330–343, https://www.researchgate.net/publication/326689809; https://ijocaas.com/wp-content/uploads/2018/07/IJOCAAS-04-03-001-June2018.pdf

[74] Ohadi M., Choo K., Dessiatoun S., Cetegen E.: *Force-Fed Microchannels for High Flux Cooling Applications*. In: Next Generation Microchannel Heat Exchangers, Chap. 2. Springer-Verlag, New York 2013, 43–60, DOI: 10.1007/978-1-4614-0779-9